Journal of Catalysis **193,** 29–39 (2000)
doi:10.1006/jcat.2000.2880, available online at http://www.idealibrary.com on IDEAL®

Surface Chemistry and Decarbonylation of Molybdenum Hexacarbonyl on Thin Alumina Films

M. Kaltchev and W. T. Tysoe[1]

Department of Chemistry and Laboratory for Surface Studies, University of Wisconsin-Milwaukee, Milwaukee, Wisconsin 53211

Received July 13, 1999; revised January 12, 2000; accepted January 28, 2000

The adsorption of molybdenum hexacarbonyl is studied on thin hydroxylated and partially hydroxylated alumina films using reflection–absorption infrared, X-ray photoelectron, and temperature-programmed desorption spectroscopies. The majority of the $Mo(CO)_6$ adsorbed on hydroxylated alumina at 80 K desorbs at ~200 K; the remainder decarbonylates leading to a molybdenum coverage of ~2% of a monolayer. Subcarbonyl species are detected as the sample is heated to ~200 K and, at higher temperatures, the molybdenum is oxidized to an ~+4 oxidation state and deposits primarily oxalate species on the surface. The adsorbed oxalates thermally decompose at ~300 K to evolve CO to form adsorbed bidentate carbonate species. These are stable to ~560 K and react to evolve CO at this temperature. The amount of molybdenum absorbed onto the surface can be increased by repeatedly dosing $Mo(CO)_6$ at 80 K and annealing to ~200 K to desorb molecular molybdenum hexacarbonyl where the molybdenum coverage increases by ~2% of a monolayer for each cycle. It is also found that the extent of decarbonylation depends on the degree of alumina hydroxylation so that heating hydroxylated alumina to 900 K, which removes ~50% of the surface hydroxyls, decreases both the CO desorption yield and the oxalate coverage by 50%.

Key Words: **alumina; thin films; molybdenum hexacarbonyl; reflection–absorption infrared spectroscopy; X-ray photoelectron spectroscopy; Auger spectroscopy; temperature-programmed desorption.**

INTRODUCTION

The growth and formation of oxide films for use, for example, as model catalyst supports have been extensively studied using a range of surface-sensitive techniques such as low-energy electron diffraction (LEED) (1), Auger and X-ray photoelectron (XPS) spectroscopies (2–4, 6), scanning-tunneling microscopy (STM) (7), high-resolution electron energy loss spectroscopy (HREELS) (3–5), and reflection–absorption infrared spectroscopy (RAIRS) (6, 10, 11) and adsorption onto these surfaces has also been investigated (8, 9, 12). Supported model catalysts have been synthesized primarily by evaporating metals or metal oxides onto these planar oxide supports to mimic "wet-impregnation" methods of catalyst preparation. Another strategy for preparing active, supported catalysts is to expose the metal oxide support to an organometallic compound which reacts with the surface to form the active catalyst. This method has been used to synthesize molybdenum catalysts that are active for olefin metathesis where the activity of the catalysts depends on the state of hydroxylation of the alumina and the temperature at which the catalyst is treated following exposure to molybdenum hexacarbonyl (13–16).

We have previously investigated the catalytic activity of molybdenum oxide films (MoO_2 and MoO_3) grown on metallic molybdenum substrates and found that they do catalyze olefin metathesis but with a substantially lower activity than that found for the most active metathesis catalysts (17). It has been shown that the activity of olefin metathesis catalysts made by reaction of molybdenum carbonyl with alumina initially increases with molybdenum loading as the number of catalytically active centers increases (18). The activity, however, subsequently decreases as the molybdenum coverage increases further. One possible explanation for this is that the active centers agglomerate at higher coverages to form a less active oxide film. This paper addresses the synthesis and characterization of model catalysts formed by the adsorption of molybdenum hexacarbonyl on planar alumina films in ultrahigh vacuum to mimic lower loading, more active metathesis catalysts.

The reaction of molybdenum hexacarbonyl with high-surface-area alumina has been previously studied extensively using temperature-programmed reaction (19, 20) and infrared spectroscopy (18, 21–24), and on planar supports using inelastic electron tunneling spectroscopy (IETS) (25). Magnetic resonance methods have also been used (26, 27). The consensus is that reaction proceeds via an initial decarbonylation step to form a stable subcarbonyl intermediate $Mo(CO)_x$. This undergoes further decarbonylation so that eventually all of the CO is removed from the system and metallic or oxidized molybdenum is left on the surface. The considerable amount of work done on the reaction of

[1] To whom correspondence should be addressed. Fax: (414) 229-5036. E-mail: wtt@csd.uwm.edu.

0021-9517/00 $35.00

$Mo(CO)_6$ with γ-alumina shows that the detailed behavior of the molecule as well as the final species formed in the catalyst's precursor strongly depends on the degree of hydroxylation of the aluminum oxide and the conditions under which the reaction proceeds (20). Results are presented in this work on the adsorption of $Mo(CO)_6$ on planar alumina grown on a Mo(100) substrate studied in ultrahigh vacuum using X-ray photoelectron and infrared spectroscopies as well as temperature-programmed desorption. In this case, the alumina film is sufficiently thin that the infrared surface intensity enhancements due to the presence of the metal substrate are maintained although it is sufficiently thick that it chemically mimics high-surface-area alumina (12).

EXPERIMENTAL

Alumina films are deposited onto a Mo(100) single-crystal substrate by sequences of cycles of aluminum evaporation/water oxidation (with D_2O, H_2O, or $H_2{}^{18}O$-enriched water) (12). These cycles are necessary to ensure complete oxidation of aluminum which may be difficult to achieve with thicker aluminum layers. Oxidation is monitored using Auger electron spectroscopy (AES) and X-ray photoelectron spectroscopy (XPS). Aluminum is evaporated from a small heated alumina tube which is enclosed in a stainless-steel shroud to minimize contamination of other parts of the system (28). It is evaporated onto a Mo(100) single crystal held at 300 K for 120 s which, from measurements of the resulting oxide film thickness, deposits ~1.5 monolayers (12).

Water is supplied via a capillary doser to minimize background contamination and the aluminum is oxidized by water vapor for 300 s with the sample held at 650 K with a background water vapor pressure of 1×10^{-8} Torr. Note that pressures are not corrected for the ionization gauge sensitivity. The local pressure in front of the dosing source is substantially higher than the background pressure. This pressure enhancement is estimated using carbon monoxide by comparing the CO dose required to saturate the clean Mo(100) surface either by backfilling the chamber or via the dosing source. In this case, CO coverages were measured from the areas under the CO temperatre-programmed desorption features (29). This shows that the dosing source provides a pressure enhancement of ~200 resulting in an effective water oxidation pressure of $\sim 2 \times 10^{-6}$ Torr when the background pressure is 1×10^{-8} Torr. The aluminum evaporation/water oxidation procedure is repeated until a film of the desired thickness is formed.

Two types of film were grown. The first is formed using water (generally with H_2O or D_2O but occasionally with ^{18}O-enriched water (10 at.%)) and annealed to 450 K to remove any remaining molecular water, yielding a surface with the maximum surface hydroxyl coverage. This sample is designated in the following as "hydroxylated alumina," or HA. Alternatively, the HA sample is annealed to 900 K to partially dehydroxylate it, leading to intermediate surface hydroxyl coverages. This is referred to as "partially dehydroxylated alumina" (PDA).

Experiments were carried out in a vacuum system that has been described in detail elsewhere (30). In the case of temperature-programmed desorption experiments, the chamber contained two aluminum evaporation sources positioned so that both the back and front faces of the Mo(100) crystal could be covered by alumina to eliminate interference due to species desorbing from the Mo(100) surface. The 12-in.-diameter, stainless-steel vacuum chamber was pumped by an ion and titanium sublimation pump and operated at a base pressure of $\sim 5 \times 10^{-11}$ Torr following bakeout. The chamber was equipped with a double-pass, cylindrical mirror analyzer for Auger and XPS analysis of the sample and a quadrupole mass analyzer for temperature-programmed desorption experiments, for leak testing, and for gauging the purity of gases introduced into the chamber. Desorption spectra were collected using a heating rate of 13 K/s. Auger spectra were collected using an electron beam energy of 3 keV and the first derivative spectrum obtained by numerical differentiation. XPS data were collected using the double-pass, cylindrical mirror analyzer operating at a pass energy of 50 eV. Mg K_α radiation was furnished by a water-cooled source operating at a power of 120 W. The chamber also contained a retractable, electron beam heating filament which is used to heat the molybdenum substrate to ~2100 K for cleaning.

RAIRS spectra were collected in another chamber which has also been described in detail elsewhere (30). Briefly, the sample was mounted to the end of a horizontal sample manipulator which could be retracted to move the sample into a small-volume infrared cell or extended to move the sample into a 12-in.-diameter analysis chamber. The sample could also be resistively heated, and cooled to ~80 K by pumping liquid nitrogen down the center of the sample transfer rod. The infrared apparatus was mounted on an optical table for stability and infrared radiation from a Midac Fourier transform spectrometer was steered and focused onto the sample. The reflected light was collected and focused onto a cooled mercury–cadmium–telluride (MCT) detector and the resulting signal collected and analyzed by a microcomputer running SpectraCalc software. The optical path was completely covered by a dry-air-purged enclosure. The infrared radiation was furnished by an air-cooled source and spectra were collected at a resolution of 4 cm^{-1} for 1000 scans which typically took 4 min to accumulate.

The oxide film was grown in the main chamber and characterized using Auger and X-ray photoelectron spectroscopies. In order to avoid potential problems due to electron beam damage of the oxide films (31), once an effective film growth protocol had been established, fresh films were

grown for infrared analysis and temperature-programmed desorption studies. Infrared spectra were collected after retracting the sample from the preparation chamber into the infrared cell. This cell was also equipped with a directional dosing source consisting of a 2-mm-diameter capillary which could be used to deposit reactants onto the sample with minimal contamination of the background. The deionized water (D_2O or H_2O) and O^{18}-labeled water ($H_2{}^{18}O$ 10 at.%, Aldrich, 95%) used to grow the films were transferred to glass vials and connected to the gas-handling line of the chamber. Normal, deionized (H_2O), or deuterated water (D_2O, Aldrich, 95%) was generally used for surface oxidation. ^{18}O-Labeled water was used in experiments to distinguish between oxygen coming from the substrate and from adorbates. The water was purified using repeated freeze–pump–thaw cycles. Molybdenum hexacarbonyl (Aldrich, 99%) was transferred to a glass vial, connected to the gas-handling line of the chamber, and purified by repeated freeze–pump–thaw cycles, followed by distillation and its purity was monitored using mass and infrared spectroscopies. This was also dosed onto the surface via a capillary doser to minimize background contamination.

RESULTS

Figure 1 displays a series of temperature-programmed desorption spectra of a monolayer of $Mo(CO)_6$ absorbed on fully hydroxylated alumina at 80 K. The calibration of the monolayer coverage is discussed in greater detail below. It should be noted that, in contrast to experiments performed on high-surface-area aluminas, no molybdenum hexacarbonyl adsorption is detected on the model oxide surfaces that were exposed to $Mo(CO)_6$ between 200 and 300 K although molybdenum is found on the surface when dosing was done at higher temperatures where molybdenum carbide is formed (32). An intense peak is noted at 205 K when monitoring 97 amu due to the desorption of molecular molybdenum hexacarbonyl (Fig. 1c) (33). The 205 K feature in the 28-amu spectrum (Fig. 1a) is assigned to a mass spectrometer ionizer fragment of the molybdenum hexacarbonyl and the intensity ratio of these TPD features agrees well with the 97/28 amu ratio measured in the mass spectrum of molybdenum hexacarbonyl (33). The contribution of the desorbing molybdenum hexacarbonyl to the 28-amu spectrum is removed by scaling the 97-amu spectrum by the ratio of the intensities of the 97- and 28-amu signals in the mass spectrum of $Mo(CO)_6$. The resulting spectrum of just CO is displayed in Fig. 1b. Due to the relatively large intensity of the 28-amu fragment from the carbonyl, it is impossible to completely exclude the possibility of a small amount of CO desorption due to decarbonylation at ~200 K. The low-temperature feature has a maximum at 310 K, and the high-temperature state is centered at 560 K. The ratio of the integrated intensities of the 560 and

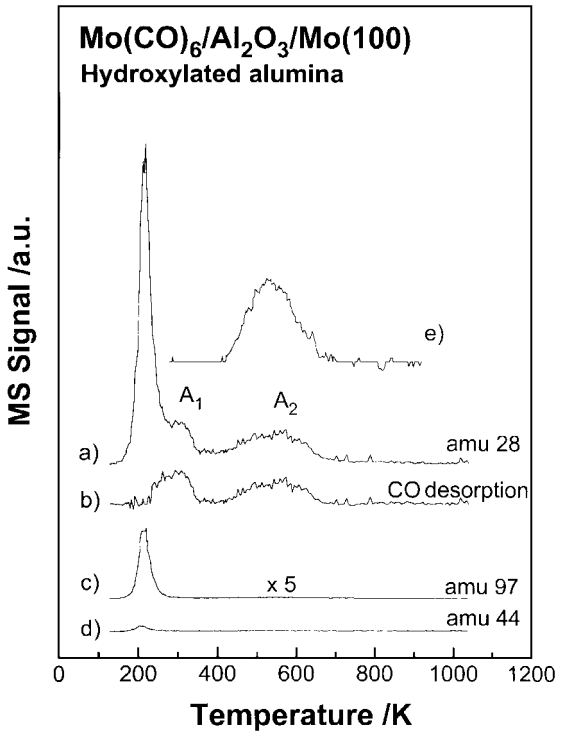

FIG. 1. Temperature-programmed desorption spectra collected at 28 (CO) (a), 97 ($Mo(CO)_6$) (c), and 44 (CO_2) (d) amu following molybdenum hexacarbonyl adsorption on alumina grown on Mo(100) by reaction between aluminum and water (H_2O) and annealed at 450 K to remove adsorbed water to yield fully hydroxylated alumina. The heating rate was 13 K/s. Shown also is the desorption spectrum of CO after subtraction of the contribution from molybdenum hexacarbonyl desorption (b) and the increase of CO desorption at 560 K after multiple carbonyl exposures (e) (see text).

310 K features is 0.90 ± 0.05 so that approximately equal amounts of CO desorb in each state. Note that, since the heating rate varies somewhat during the desorption sweep, these measurements were made by integrating the peak areas over time rather than temperature to yield an accurate measurement of the relative coverages. The total amount of CO desorbing in these states can be gauged by comparing it with the CO desorbing from the clean Mo(100) substrate where, since the oxide is grown on this substrate, the sample areas are exactly identical and, in each case, exactly identical experimental protocols were used to collect TPD data. Taking into account that each $Mo(CO)_6$ contains six carbons reveals that these states account for the adsorption of $2.0 \pm 0.1\%$ of a monolayer of molybdenum.

In order to establish whether decarbonylation takes place at some special sites, the following experiment was carried out. A fully hydroxylated alumina sample was exposed to $Mo(CO)_6$ at 80 K, and warmed to 300 K to desorb all molecular species. Note that, since this sample was previously heated to 450 K to remove molecular water, this procedure will not alter the state of hydroxylation of the sample. The

sample was once again saturated with $Mo(CO)_6$ at 80 K and again annealed to 300 K, and this procedure was repeated six times. A temperature-programmed desorption experiment was then carried out monitoring the 28- and 97-amu signals. No molybdenum hexacarbonyl (at 97 amu) desorbed from the surface as expected since this had been removed from the sample during annealing. The 560 K TPD signal at 28 amu was, however, 6 times larger (Fig. 1e) than the corresponding signal shown in Figs. 1a and 1b. This indicates that hexacarbonyl decarbonylation does not take place at special sites on the alumina surface but that there is a branching reaction between hexacarbonyl desorption and decarbonylation with carbonyl desorption predominating. Finally, as shown in Fig. 1d, the 44-amu signal (CO_2) is very weak and can be assigned to a small contribution from the hexacarbonyl. In addition, no hydrogen desorption was detected.

The corresponding TPD spectra for $Mo(CO)_6$ adsorbed on partially dehydroxylated alumina (which had been heated to 900 K *in vacuo*) are displayed in Fig. 2. The main features of these spectra resemble those for molybdenum hexacarbonyl adsorbed on hydroxylated alumina

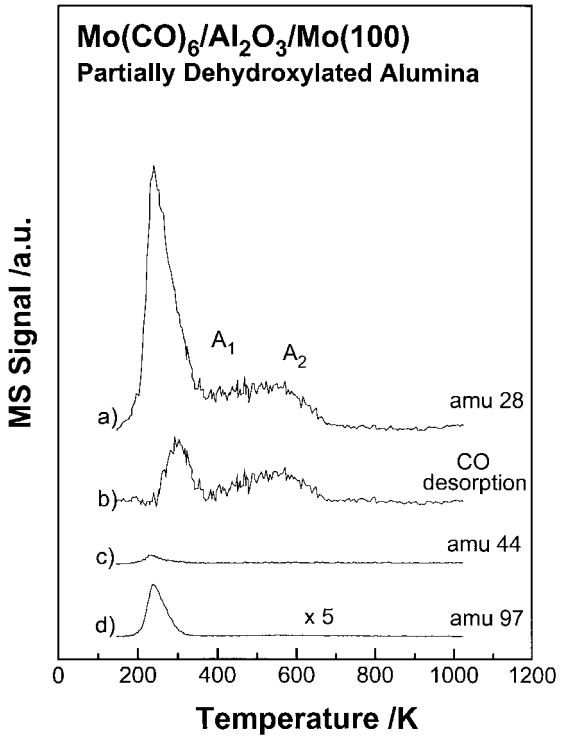

FIG. 2. Temperature-programmed desorption spectra collected at 28 (CO) (a), 97 ($Mo(CO)_6$) (d), and 44 (CO_2) (c) amu following molybdenum hexacarbonyl adsorption on alumina grown on Mo(100) by reaction between aluminum and water (H_2O) and annealed at 900 K to remove a portion of the surface hydroxyls to yield partially dehydroxylated alumina. Data were collected at a heating rate of 13 K/s. Shown also is the desorption spectrum of CO after subtraction of the contribution from molybdenum hexacarbonyl desorption (b).

TABLE 1

Comparison of the Properties of Hydroxylated Alumina (HA) with Those of Partially Dehydroxylated Alumina (PDA)

Sample	HA	PDA
Relative hydroxyl coverage from TPD	1	0.5 ± 0.1
Relative CO TPD yield	1	0.57 ± 0.03
Relative intensity of 1290 cm^{-1} RAIRS feature (oxalate species)	1	0.5 ± 0.1

(Fig. 1) except that the desorption states are less well resolved. Molybdenum hexacarbonyl desorbs at a slightly higher temperature (230 K) than on hydroxylated alumina. There is a clearly discernible 560 K CO desorption feature which is somewhat broader than that on the fully hydroxylated sample. The lower-temperature feature is partially obscured by the 28-amu fragment of the molybdenum hexacarbonyl, but this can again be resolved by subtracting the carbonyl contribution which is gauged from its 97-amu signal. The resulting spectrum due to CO desorption is also displayed in Fig. 2b. This yields features centered at 310 and 560 K and the relative intensity ratio $I(560\ K)/I(300\ K)$ is 0.9 ± 0.1, so that again, approximately equimolar amounts of CO desorb in each state. No CO_2 or hydrogen is found to desorb from this surface. The relative degree of hydroxylation is measured from the total H_2O (18 amu) desorption yield in temperature-programmed desorption immediately following sample preparation. Water desorbs from the model oxide in a relatively broad and featureless distribution. The sample was heated to a maximum temperature of 1280 K to ensure complete dehydroxylation of the alumina. The results of this experiment reveal that the hydroxyl coverage of the partially dehydroxylated surface is 0.5 ± 0.1 of that of the fully hydroxylated sample so that approximately 50% of the surface hydroxyls are removed by annealing to 900 K (see Table 1). Table 1 also compares the total CO desorption yield (the sum of the low- and high-temperature CO desorption states) for fully and partially hydroxylated surfaces. This reveals that only 0.57 ± 0.03 of the amount of CO desorbs from the partially dehydroxylated surface as from the fully hydroxylated surface. This ratio agrees well with the relative hydroxyl coverage and suggests that decarbonylation is associated with the presence of surface hydroxyl species. This suggests that the remaining molybdenum coverage on the partially hydroxylated alumina following desorption of molecular $Mo(CO)_6$ is 1.15 ± 0.10% of a monolayer. Dependencies on decarbonylation behavior of $Mo(CO)_6$ on the extent of hydroxylation by hydroxylated alumina have been noted previously (20).

The total CO desorption yield from fully hydroxylated alumina varies with hexacarbonyl coverage as demonstrated by the plot in Fig. 3. Since $Mo(CO)_6$ is dosed

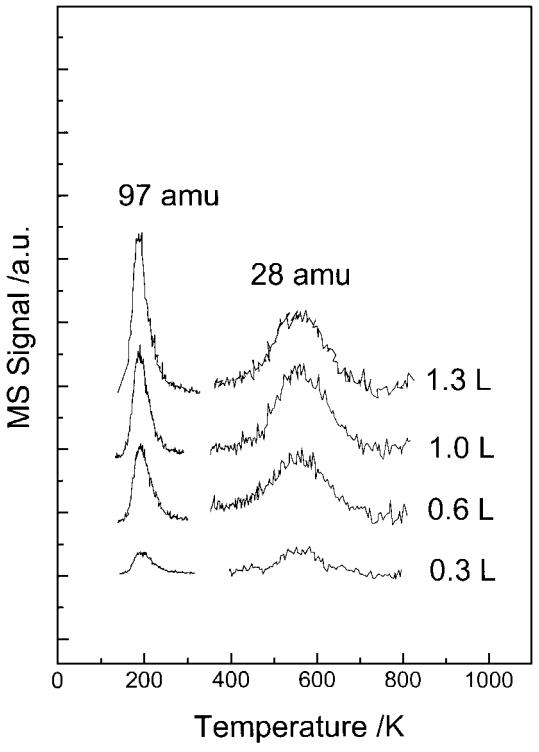

FIG. 3. TPD spectra of 97 amu and 28 amu used to build the curve in Fig. 4. For clarity, only the high-temperature CO desorption peak is shown.

using the directional doser, exposures are calculated from the increase in background pressure using the enhancement factor calculated for carbon monoxide (∼200, see Experimental section). Pressures are also not corrected for the ionization gauge sensitivity. Since the majority of the $Mo(CO)_6$ desorbs, the integrated intensity of the 97-amu signal is taken to be a gauge of the initial carbonyl coverage rather than using Auger or X-ray photoelectron spectroscopy since X-ray and electron beams induce carbonyl decomposition (see below). The variation in CO yield with hexacarbonyl coverage is illustrated in Fig. 4, where the desorption yield of CO is plotted versus the desorption yield of molecular $Mo(CO)_6$ (97 amu). The CO desorption yield increases with increasing carbonyl coverage and saturates at a carbonyl desorption yield of 80 arbitrary units (a.u.) (corresponding to a carbonyl exposure of 0.6 L) and remains constant thereafter. Similar results are found for the partially dehydroxylated samples and the TPD spectra shown in Figs. 1 and 2 above were collected for the saturation of the monolayer (at 80 a.u. $Mo(CO)_6$ desorption yield for both hydroxylated and dehydroxylated surfaces). It should be noted that the peak positions in the temperature-programmed desorption spectra do not change with variations in dose; only their relative intensities change.

In order to establish whether the 310 and 560 K CO desorption states (Figs. 1 and 2) are due to the desorption of intact CO or whether they are preceded by dissociation, temperature-programmed desorption spectra were collected from a hydroxylated alumina surface that was prepared from ^{18}O-enriched H_2O. In this case, any CO dissociation will deposit carbon onto the surface which would then recombine with isotopically labeled oxygen on the surface to desorb $^{12}C^{18}O$ (30 amu). No 30-amu signal was detected following this experiment, confirming that the CO molecules remain intact (Fig. 5).

It has been found previously that partially decarbonylated molybdenum carbonyl species (for example, $Mo(CO)_{3(ads)}$) present on high-surface-area alumina can be recarbonylated by pressurizing with CO (21). Attempts were made to recarbonylate a hydroxylated alumina surface exposed to $Mo(CO)_6$ and heated to between 250 K and 1200 K using a 3-L CO exposure ($1\ L = 1 \times 10^{-6}$ Torr · s) at a sample temperature of 80 K. A small amount of CO desorption was detected at ∼160 K due to CO adsorbing weakly on the alumina surface (34, 35) with no signal detected at higher temperatures, indicating that no recarbonylation of the carbonyl-derived species took place.

X-ray photoelectron spectroscopy was used to monitor the coverage and oxidation state of the molybdenum on the surface. It was found that molybdenum hexacarbonyl adsorbed at 80 K was very sensitive to the X-ray beam since a rapid decrease in the intensity of the molybdenum

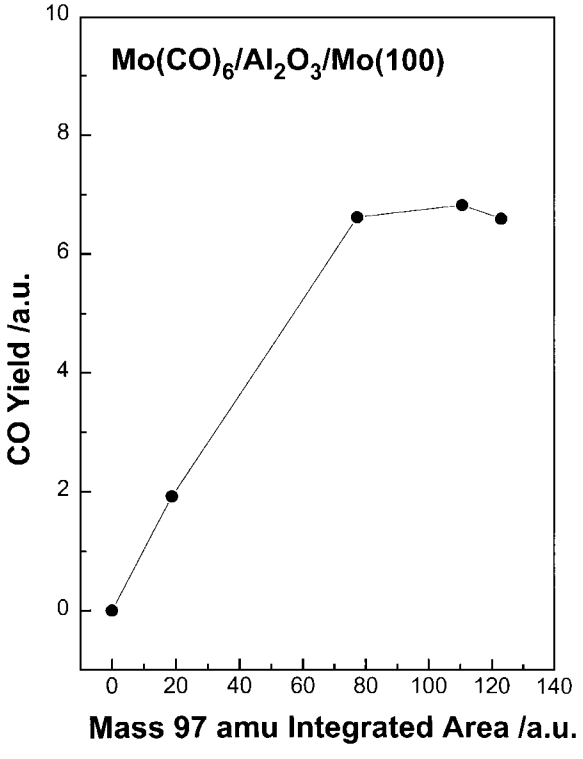

FIG. 4. Plot of the total CO yield in temperature-programmed desorption versus the molybdenum carbonyl coverage monitored from the molybdenum carbonyl desorption yield measured from the 97 amu TPD signal.

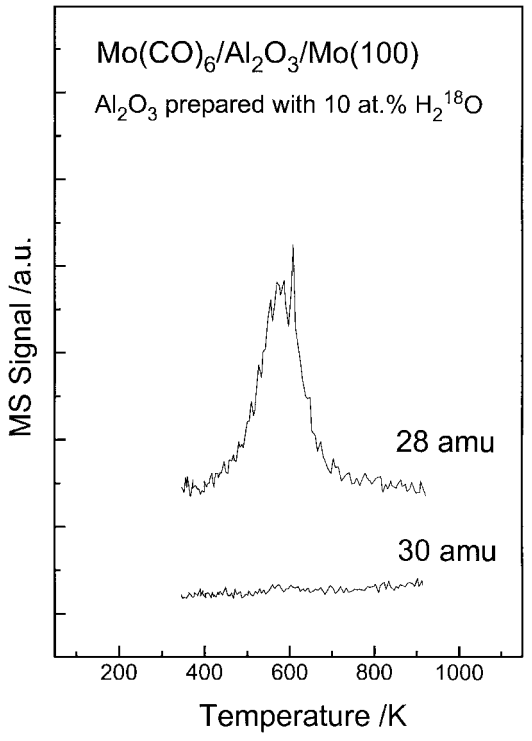

FIG. 5. TPD spectra of 28 amu and 30 amu after desorption of $Mo(CO)_6$ adsorbed on alumina prepared with H_2O containing 10 at.% $H_2{}^{18}O$. Again, for clarity only the peak at 560 K is shown.

signal was noted due to the incident X-ray flux. It was found, however, that the spectra of molybdenum species formed by adsorbing at 80 K and heating to above 250 K were stable in the X-ray beam and no changes in the intensity or position of the Mo 3*d* feature were found as a function of X-ray dose, although X-ray-induced reduction of MoO_3 has been noted by other workers (31). As found above, measurements of the CO desorption yields reveal that the coverage of molybdenum deposited onto hydroxylated alumina by adsorbing $Mo(CO)_6$ at 80 K and annealing to desorb molecular carbonyls is rather low (~2% of a monolayer). In order to increase the surface molybdenum coverage to allow photoelectron spectra to be collected, the surface was saturated with $Mo(CO)_6$ and annealed to 205 K. The sample was then cooled to 80 K and redosed and once again annealed to 205 K. This procedure was repeated a total of eight times (to produce, according to the measured CO desorption yield, a total molybdenum coverage of ~0.16 monolayer) and the X-ray photoelectron spectrum recorded. Typical X-ray photoelectron spectra recorded for 1000 scans for a sample subsequently annealed to 275, 525, and 670 K are shown in Fig. 6. The alumina film is grown on a Mo(100) single crystal. The film was sufficiently thick to obscure signals from the substrate and the baseline spectrum prior to molybdenum hexacarbonyl adsorption is displayed in Fig. 6a. The Mo 3*d* spectrum consists of relatively broad features centered at 231.3 ± 0.1 and 234.5 ± 0.1 eV binding energies.

Figure 7 displays the corresponding set of infrared spectra for molybdenum hexacarbonyl adsorbed at 80 K on hydroxylated alumina grown using deuterated (D_2O) water. These spectra are collected after annealing *in vacuo* to the temperature indicated adjacent to each spectrum for 5 s, following which the sample was allowed to cool to 80 K and the spectrum recorded. The absorbance scale is indicated as a vertical line on the figure. A monolayer of molybdenum carbonyl adsorbed on alumina at 80 K exhibits a single peak at 2040 cm^{-1} due to unperturbed $Mo(CO)_6$. Annealing to 185 K shifts the peak slightly and the nature of the surface species formed in the intervening temperature range up to 205 K on partially dehydroxylated alumina will be discussed in greater detail below. Heating to 205 K removes all of the sharp carbonyl modes at ~2000 cm^{-1}. Several relatively broad features develop at ~1900 cm^{-1}, at between 1580 and 1660 cm^{-1}, and at 1290 cm^{-1} with a shoulder at ~1345 cm^{-1} with a broad peak apparent at 1020 cm^{-1}. Sharper peaks appear at 1720 and 1130 cm^{-1}. The spectrum also displays a negative feature at ~920 cm^{-1}. The reference spectrum for these data are clean,

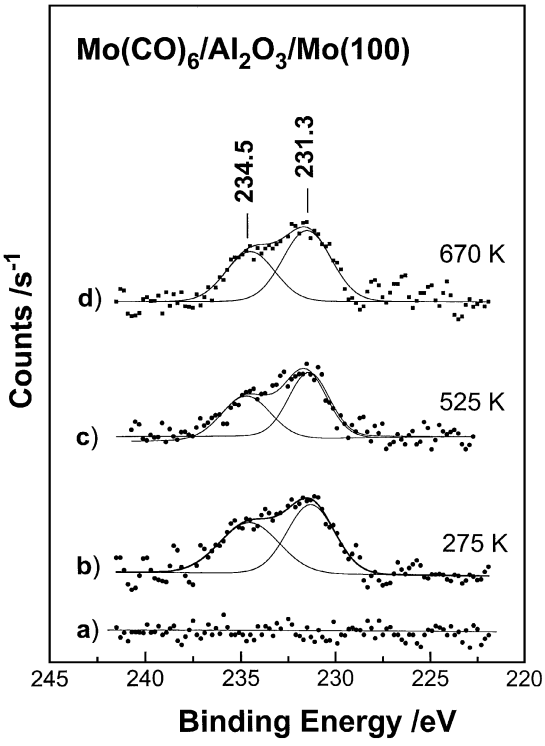

FIG. 6. Mo 3*d* X-ray photoelectron features from $Mo(CO)_6$ adsorbed onto hydroxylated alumina at 80 K and annealed to 205 K to remove molecular hexacarbonyl. The surface was then redosed at 80 K and annealed to 205 K to deposit additional molybdenum hexacarbonyl and this procedure was carried out a total of eight times. This spectrum was collected after the sample was heated to 275 K for 5 s and allowed to cool to 80 K (b). Shown also are the spectra of the surface after subsequent heating to 525 (c) and 670 K (d) as well as the spectrum of the alumina sample in the Mo 3*d* region prior to reaction with $Mo(CO)_6$ (a).

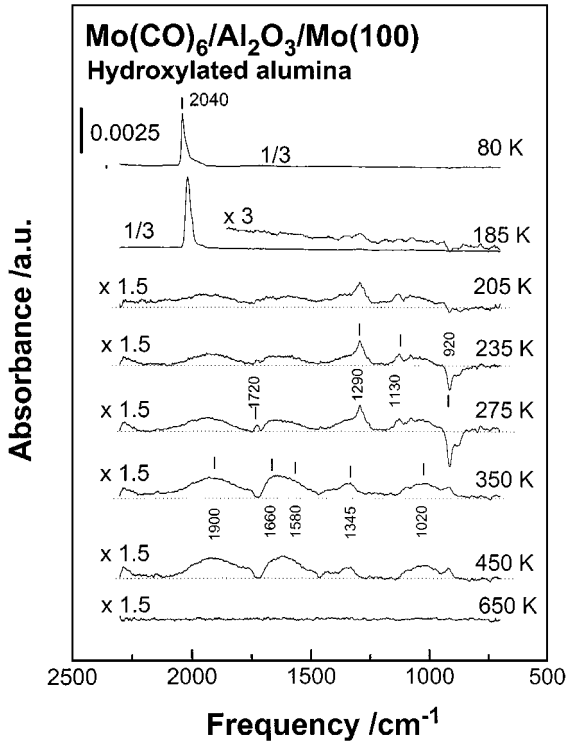

FIG. 7. Reflection–absorption infrared spectra of alumina grown on Mo(100) by reaction between aluminum and water (D_2O) and annealed at 450 K to remove adsorbed water to yield fully hydroxylated alumina and then exposed to $Mo(CO)_6$ at 80 K and annealed to various temperatures. Annealing temperatures are marked adjacent to the corresponding spectrum. The absorbance scale is indicated by a vertical line on the figure. A dashed line indicates the baseline.

alumina-covered Mo(100) surfaces. The alumina itself exhibits lattice modes at ~920 cm^{-1} (6) so that this decrease is ascribed to a quenching of the alumina lattice modes by carbonyl adsorption. The main features of this spectrum persist up to an annealing temperature of 275 K and the intensities of the 1720, 1290, and 1130 cm^{-1} features remain relatively constant whereas the broad 1580–1660 and 1020 cm^{-1} features grow slightly.

Upon further heating of the surface to ~350 K, part of the CO desorbs (Fig. 1). This is accompanied by the disappearance of the sharp 1720, 1290, and 1130 cm^{-1} modes. Simultaneously, the broad feature between 1580 and 1660 cm^{-1} as well as the 1020 cm^{-1} feature increases substantially in intensity. This suggests that the surface species responsible for peaks at 1720, 1290, and 1130 cm^{-1} decomposes to desorb CO at ~300 K and yield a species exhibiting a broad peak between 1660 and 1580 cm^{-1} and a peak at 1020 cm^{-1}. The peak originally present as a shoulder at 1345 cm^{-1} appears to maintain a constant intensity. The 1900 cm^{-1} feature grows continually in intensity during annealing. All of the surface modes disappear on heating of the surface to 650 K, corresponding to the removal of the remaining CO from the surface (Fig. 1).

The spectra displayed in Fig. 7 were collected for $Mo(CO)_6$ adsorbed on hydroxylated alumina prepared using D_2O. Carrying out a similar experiment on a surface prepared using H_2O yields a very similar spectral series as displayed in Fig. 8. This result indicates that all of the vibrational modes involve carbon and oxygen.

Figure 8 displays a series of infrared spectra of molybdenum hexacarbonyl adsorbed onto alumina grown using H_2O and partially dehydroxylated by heating to ~900 K. Again, the spectra are collected after annealing *in vacuo* to the temperature indicated adjacent to each spectrum for a period of 5 s, after which the sample is allowed to cool to 80 K and the spectrum recorded. The absorbance scale is indicated as a vertical line on the spectrum. Immediately following adsorption at 80 K, the spectrum exhibits three features at 2033, 2012, and 1964 cm^{-1}. The gas-phase infrared spectrum of molybdenum carbonyl has a single feature at 2003.0 cm^{-1} (36) which is assigned to the t_{1u} CO stretching mode of the carbonyl. The corresponding a_{1g} and e_g modes are symmetry forbidden in infrared but are detected at 2117 and 2019 cm^{-1}, respectively, using Raman spectroscopy. The features found for the monolayer are substantially perturbed from those for gas-phase $Mo(CO)_6$, indicating an

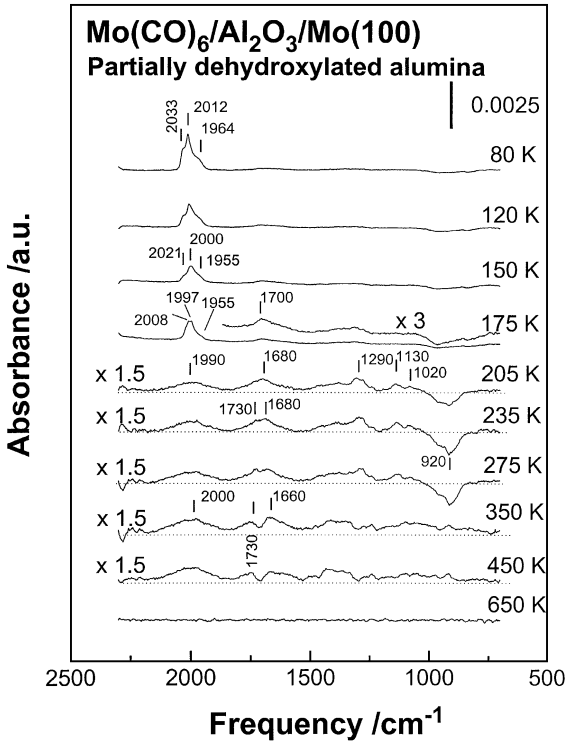

FIG. 8. Reflection–absorption infrared spectra of alumina grown on Mo(100) by reaction between aluminum and water (H_2O) and annealed at 900 K to remove a portion of the surface hydroxyls and exposed to $Mo(CO)_6$ at 80 K and annealed to various temperatures. Annealing temperatures are marked adjacent to the corresponding spectrum. The absorbance scale is indicated by a vertical line on the figure. A dashed line is shown to indicate the baseline.

interaction with the surface. The spectrum changes as the surface is heated to 120 and 150 K, so that at 150 K, the spectrum consists of lines at 2021, 2000, and 1955 cm^{-1} with a broad feature emerging at 1700 cm^{-1}. Brown *et al.* (23) have identified $Mo(CO)_{5(ads)}$ species on partially deydroxylated and hydroxylated alumina from their infrared features at 2028 and 1998 cm^{-1} with a shoulder at 1950 cm^{-1}, in good agreement with the spectrum observed on annealing to 150 K (Fig. 8) Additional broad features detected at 1850 and 1790 cm^{-1} have been associated with interactions with Type I Lewis acid sites (1850 cm^{-1}) and with sites of Type II (1790 cm^{-1}) (23). The broad feature at ~1700 cm^{-1} may be associated with this interaction.

On heating of the surface to ~175 K, the spectrum in the carbonyl stretching regions shifts to slightly higher frequencies and exhibits two closely spaced peaks of almost identical intensity at 2008 and 1997 cm^{-1} with a shoulder at approximately 1955 cm^{-1}. The uncertainty in this last figure is relatively large as it is only present as a shoulder. The broad feature persists at ~1700 cm^{-1}. Reddy and Brown have observed a similar spectrum following adsorption of $Mo(CO)_6$ on alumina which was assigned to the presence of relatively stable adsorbed $Mo(CO)_3$ species (23), where the 1700 cm^{-1} mode is again assigned to the interaction of one of the CO ligands with an adjacent aluminum.

Again, the most drastic spectral changes are evident on heating to 205 K. The sharp carbonyl stretching modes are completely absent although there is a broad feature at ~1990 cm^{-1} and the spectrum consists of main features at 1680 and 1290 cm^{-1} with less intense peaks at 1130 cm^{-1}. The negative excursion in the region 800 to 1000 cm^{-1} is also detected but is broader than that on hydroxylated alumina and is again assigned to an attenuation of the substrate lattice modes. This spectrum persists on annealing to 275 K *in vacuo* except that the 1730 cm^{-1} peak becomes more clearly defined. These features are essentially identical to those found on fully hydroxylated alumina (Fig. 7). Note, however, that the intensities of the features on partially dehydroxylated alumina (Fig. 8) are lower than those on the fully hydroxylated sample (Fig. 7). The relative intensities of the 1290 cm^{-1} feature (assigned below to an oxalate species) are compared in Table 1 for hydroxylated and partially dehydroxylated alumina. The relative intensity of this feature agrees well with the relative degree of hydroxylation, suggesting that this species is formed by interaction with surface hydroxyl species. It also agrees well with the relative CO thermal desorption yield. Further heating to 350 K results in substantial changes to the spectrum similar to those found on hydroxylated alumina (Fig. 7). These changes are accompanied by CO desorption (Fig. 2). The intensity of the spectrum is lower than that on hydroxylated alumina and the spectrum again exhibits a broad feature between 1580 and 1660 cm^{-1} with a slightly enhanced intensity at ~1020 cm^{-1}. The 2000 cm^{-1} feature persists and the 1345 cm^{-1} feature noted on hydroxylated alumina is approximately equal in intensity to the 1580–1660 cm^{-1} peak on partially hydroxylated alumina whereas on the hydroxylated surface the 1580–1660 cm^{-1} peak is significantly more intense.

DISCUSSION

Previous studies of $Mo(CO)_6$ decarbonylation have been carried out primarily using high-surface-area substrates either in the presence of the CO evolved from the surface (20) or under relatively modest vacuums (22–24) and by IETS on planar supports (25). It has also been clearly demonstrated that surface subcarbonyls can recarbonylate when exposed to an external pressure of CO (21). In contrast, in ultrahigh vacuum, any CO evolved from the surface is completely removed so that it is likely that $Mo(CO)_6$ decarbonylates at lower temperatures in UHV than on high-surface-area samples. There is nevertheless a strong similarity between the temperature-programmed desorption data found on planar substrates (Figs. 1 and 2) and high-surface-area alumina (37). Thus, two CO desorption states are detected at 388 and 596 K for $Mo(CO)_6$ adsorbed at 300 K on γ-alumina using a heating rate of 0.167 K/s. Two states are also detected on fully and partially hydroxylated, planar substrates at 310 and 560 K when adsorbed at 80 K using a heating rate of 13 K/s (Figs. 1 and 2, respectively). A full analysis of the desorption data on high-surface-area alumina yields a decarbonylation activation energy of 109 kJ/mol for the first state and 170 kJ/mol for the second (37). A Redhead analysis of the data for high-surface-area alumina yields values of 110 and 171 kJ/mol for the first and second states, respectively, assuming a preexponential factor of 10^{13} s^{-1} (38). A corresponding Redhead analysis of the TPD spectra for the planar samples in Figs. 1 and 2, assuming the same preexponential factor (10^{13} s^{-1}), yields values of 76 and 141 kJ/mol for the first and second states, respectively. The higher value for the low-temperature state for $Mo(CO)_6$ adsorbed on high-surface-area alumina likely arises since some CO already desorbs at room temperature so that the 388 K feature on high-surface-area alumina represents the high-temperature portion of this state. The agreement between the values for the high-temperature states is much better and is within ~30 kJ/mol. The slightly higher activation energy found on γ-alumina may be due to some recarbonylation of the carbonyl arising from the presence of some gas-phase CO, as noted above (21).

Adsorbed molybdenum hexacarbonyl decarbonylates on planar alumina supports at relatively low temperatures via an intermediate pentacarbonyl species formed between 130 and 160 K and the formation of adsorbed $Mo(CO)_3$ at ~175 K (Fig. 8). As noted above, the species formed on partially dehydroxylated alumina at 80 K (Fig. 8) exhibits features at 2033, 2012, and 1964 cm^{-1} that are assigned to

$Mo(CO)_{5(ads)}$ (23). The species formed on heating to 175 K (Fig. 8) shows features at 2008, 1997, and 1955 cm^{-1} that are assigned to an $Mo(CO)_{3(ads)}$ species (23). These assignments are in agreement with the conclusions of Reddy and Brown on high-surface-area alumina (23) although these decarbonylation temperatures are somewhat lower than in the case of high-surface-area alumina, presumably since CO is more rapidly removed in ultrahigh vacuum.

The most drastic changes take place, both on hydroxylated (Fig. 7) and partially dehydroxylated (Fig. 8) alumina, on heating to 205 K, yielding an array of features between 1000 and 2000 cm^{-1} which persists up to 275 K.

The XPS spectrum of the surface at 275 K shows features centered at 231.3 ± 0.1 and 234.5 ± 0.1 eV binding energies (Fig. 6b). The spectra collected after annealing to 525 K (Fig. 6c) and 670 K (Fig. 6d) are identical. The spacing between these features (3.2 ± 0.2 eV) agrees well with the spin–orbit splitting energy between the $3d_{5/2}$ and $3d_{3/2}$ features for molybdenum (39). The line shown fitted to these data is a combined Gaussian/Lorentzian line shape assuming a single component for each feature. The chemical shift of this peak corresponds to molybdenum in an approximately +4 oxidation state, indicating that the molybdenum has been substantially oxidized on the surface (40–43). Note that it may be possible to fit two or more narrower components to this profile but this is not warranted by the noise level of the data. It should be emphasized that care was taken to grow a sufficiently thick oxide layer by repeated exposure to aluminum and water that the intensity from the substrate molybdenum was completely suppressed and the spectrum prior to carbonyl adsorption is shown in this figure (Fig. 6a).

The integrated area under the Mo 3*d* XPS signal is proportional to the molybdenum coverage. We have shown that molybdenum reacts with an alumina surface when the sample is heated to 700 K to deposit a carbided molybdenum layer (32). There is a break in the amount of molybdenum deposited onto the surface of alumina as a function of carbonyl dose, monitored using Auger spectroscopy, that is taken to correspond to the formation of a molybdenum monolayer (32). The molybdenum 3*d* signal from this surface is used to calibrate the molybdenum XPS signal shown in Fig. 6 and reveals that this corresponds to $13 \pm 3\%$ of a monolayer of molybdenum. Since this was formed in eight repeated depositions of $Mo(CO)_6$, each layer corresponds to the formation of $1.6 \pm 0.3\%$ of a monolayer of molybdenum. This value is very close to the amount of molybdenum deposited onto the surface as gauged from the total CO TPD yield ($2.0 \pm 0.1\%$, see above) and implies that essentially all of the molybdenum on the surface is oxidized to Mo^{4+} after heating to above 250 K. This conclusion is in accord with the observation that the molybdenum cannot be recarbonylated since it has no coordinately unsaturated sites.

The broad features at ~1900 cm^{-1} in the infrared spectrum of hydroxylated alumina (Fig. 7) and at ~2000 cm^{-1} on partially dehydroxylated alumina (Fig. 8) are likely due to some CO that remains coordinated to the molybdenum. Since the molybdenum is present in an ~+4 oxidation state, this can be represented as an $MoO_2(CO)_x$ species. This is strikingly similar to a proposal by Brenner and Burwell (20) who suggested an oxidized molybdenum species incorporating two CO molecules so that $x = 2$.

We initially turn our attention to the surface species formed between 350 and 450 K on hydroxylated alumina (Fig. 7). Heating the sample to ~350 K desorbs ~50% of the adsorbed CO (Fig. 1) to yield a spectrum with an asymmetric feature between 1580 and 1660 cm^{-1} with a broad peak at 1020 cm^{-1} (Fig. 7). An additional relatively small feature is detected at ~1345 cm^{-1}. Note that the small peak at 920 cm^{-1} corresponding to the dip at this frequency in the 235 and 275 K spectra in Fig. 7 is assigned to quenched alumina lattice modes. Since no shifts are observed in the 1580–1660, 1345, and 1020 cm^{-1} modes on deuteration, these modes all involve carbon and oxygen vibrations. In addition, since they are formed after desorption of 50% of the total carbon monoxide, the surface species formed between 250 and 450 K contain half of the CO entities as that present between 205 and 275 K. It is proposed that the low-temperature species contain two CO units and the high-temperature species just one. Furthermore, since the extent of decarbonylation increases with the extent of surface hydroxylation (Table 1), the surface species likely involve surface OH species. A relatively large number of carbon- and oxygen-containing species have been identified on surfaces (44) and as organometallic complexes (45–48). The closest correspondence to the observed features is for a bidentate carbonate complex which can be envisaged as a CO species coordinated to two surface oxygens. The assignments are summarized in Table 2 where the irreducible representations are given for C_{2v} symmetry with the C=O axis of the coordinated CO species oriented perpendicularly to the surface. The agreement between the a_1 ν(C=O) and ν(C–O) modes at 1580–1660 and 1020 cm^{-1}, respectively, and the corresponding model compounds is extremely good. There is no intensity between 1260 and 1290 cm^{-1}

TABLE 2

Assignment of the Vibrational Spectrum of the Species Formed by Exposure of $Mo(CO)_6$ to Hydroxylated Alumina at 80 K and Heated to between 350 and 450 K

Assignment	$Mo(CO)_6$/HA, 350–450 K	Co(III) complex (47)	Nakamoto (46)
ν(C=O), a_1	1580–1660	1595	1590–1640
ν(C–O), b_2	—	1265	1260–1290
	1345	—	—
ν(C–O), a_1	1020	1030	1030

TABLE 3

Assignment of the Vibrational Spectrum of the Species Formed by Exposure of $Mo(CO)_6$ to Hydroxylated Alumina at 80 K and Heated to between 205 and 275 K

Assignment	$Mo(CO)_6$/HA	$CO_2/\sqrt{3}$ K/Ru (44)	$K_2C_2O_4$ (44)	$C_2O_4^=$ (48)	Nakamoto (46)
ν_s(OCO), b_2	1720	1716	1650	1555	1650–1700
ν_s(OCO), a_1	1290	1342	1308	1308	1250–1400
δ(OCO), a_1	1130	806	766	766	900

in the spectra of Fig. 7 which would correspond to the b_2 ν(C–O) mode. This peak may be shifted to 1345 cm^{-1} but the correspondence between the model compounds and the surface species suggests that it should not be substantially shifted. In addition, the relative intensity of the 1345 cm^{-1} feature compared to that at 1580–1600 cm^{-1} is larger on partially dehydroxylated alumina (Fig. 8). The most likely explanation for the absence of the b_2 mode in the spectra of Fig. 7 is that the bidentate species maintains its C_{2v} symmetry on the surface so that only modes of a_1 symmetry are detected. Since the 1345 cm^{-1} feature is relatively more intense on a partially dehydroxylated surface (Fig. 8), this may be due to a species analogous to a bidentate carbonate but with the carbon bonded to an aluminum. This would produce a surface carboxylate species which is characterized by bands at 1300–1450 and 1500–1680 cm^{-1} (45). The observed frequency of 1345 cm^{-1} is within the range of the first band and a portion of the broad peak at between 1580 and 1660 cm^{-1} may include contributions from the higher frequency band of a carboxylate. The presence of bulk carbonates also cannot be ruled out (44, 49). Note, finally, that, while the bidentate carbonate species predominates above 300 K on hydroxylated alumina, some of these species are also present on the surface at lower temperatures.

At lower temperatures (between 205 and 300 K) on hydroxylated alumina, a species is found that exhibits relatively sharp features at 1720, 1290, and 1130 cm^{-1}. This decomposes above 300 K to evolve CO and yield a bidentate carbonate complex so that it is proposed to contain two CO units. It is assigned to the presence of an oxalate species and the assignments are shown in Table 3, where the irreducible representations are given assuming that the adsorbate has C_{2v} symmetry with the oxalate plane perpendicular to the surface with the C–C linkage parallel to it. If this were strictly true, the b_2 mode (at 1720 cm^{-1}) should be symmetry forbidden whereas it is evident although rather weak. This suggest that the oxalate plane is slightly tilted with respect to the surface normal. The mode observed at 1130 cm^{-1} is higher in frequency than that found for model compounds and this mode may be stiffened by bonding to the surface. Note also that facile carbon–carbon coupling to form oxalate species has been previously observed on surfaces (44). It should also be emphasized that these species are not observed for CO adsorbed on alumina where it bonds rather weakly (34, 35) but is apparently induced by the transfer of CO from the carbonyl to the alumina surface. It should be noted that the modes observed between 1000 and 2000 cm^{-1} cannot be accounted for by species derived from molybdenum, aluminum, and oxygen since vibrations for these species appear at lower frequencies (<1000 cm^{-1}) (6, 50). The postulated surface species and their properties are summarized in Table 4 and the proposed chemistry for the oxalate species formed from $Mo(CO)_6$ decomposition on alumina is summarized as

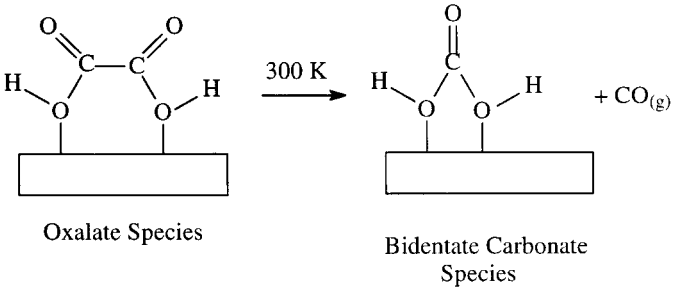

where the oxalate species formed at ~200 K thermally decomposes at ~300 K to form a bidentate carbonate and desorb CO. This thermally decomposes at ~560 K also yielding CO.

TABLE 4

Properties of Surface Species Identified on Alumina Following Adsorption of Molybdenum Hexacarbonyl

Species	Frequencies/cm^{-1}	Temperature range/K	Decomposition activation energy/kJ/mol
$Mo(CO)_5$	2033, 2012, 1964, 1700	80–150	—
$Mo(CO)_3$	2021, 2000, 1955, 1701	160–180	—
Oxalate species	1720, 1290, 1130	205–275	76
Bidentate carbonate species	1660–1580, 1020	300–560	141
$MoO_2(CO)_x$	~1920 on HA, ~2000 on PDA, XPS peaks at 231.3 and 234.5 eV BE	205–560	—

CONCLUSIONS

Molybdenum hexacarbonyl adsorbs on hydroxylated alumina films grown on a molybdenum substrate at 80 K with the majority of the adsorbed hexacarbonyl desorbing intact at ~200 K, with only ~2% reacting with the surface on fully hydroxylated alumina. Additional molybdenum can be adsorbed on the surface by redosing at 80 K and heating, indicating that this is a kinetically limited process rather than decomposition at particular sites on the surface. Decarbonylation of the adsorbed carbonyl is found between 80 and 175 K where intermediate adsorbed $Mo(CO)_5$ and $Mo(CO)_3$ species are identified. Drastic changes in the nature of the surface species are found on heating to ~205 K where oxalate and $MoO_2(CO)_x$ species are proposed to form. The $MoO_2(CO)_x$ is thermally stable up to at least 450 K and the adsorbed oxalate species thermally decomposes at ~300 K to form a bidentate carbonate species which subsequently reacts at ~560 K to evolve the remainder of the CO, accounting for the equimolar amounts of carbon monoxide desorbing at ~300 and 560 K.

ACKNOWLEDGMENTS

We gratefully acknowledge partial support of this work by the U.S. Department of Energy, Division of Chemical Sciences, Office of Basic Energy Sciences, under grant number DE-FG02-92ER14289. We also thank Professor J. J. Fripiat for useful discussions.

REFERENCES

1. Chen, P. J., and Goodman, D. W., *Surf. Sci.* **312**, L767 (1994).
2. Madden, H. H., and Goodman, D. W., *Surf. Sci.* **150**, 39 (1985).
3. Chen, P. J., Goodman, D. W., and Yates, Jr., J. T., *Phys. Rev. B* **41**, 8025 (1990).
4. Frederick, B. G., Apai, G., and Rhodin, T. N., *Surf. Sci.* **244**, 67 (1991).
5. Rhodin, T. N., Frederick, B. G., and Apai, G., *Surf. Sci.* **287**, 638 (1993).
6. Brüesch, C., Kötz, R., Neff, N., and Pietronero, L., *Phys. Rev. B* **29**, 4691 (1984).
7. Xu, C., Oh, W. S., Liu, G., Kim, D. Y., and Goodman, D. W., *J. Vac. Sci. Technol. A* **15**(3), 1261 (1997).
8. Rhodin, T. N., Merril, R. P., O'Hagan, P. J., Woronick, S. C., Shinn, N. D., Woolery, G. L., and Chester, A. W., *J. Phys. Chem.* **98**, 2433 (1994).
9. Frederick, B. G., Apai, G., and Rhodin, T. N., *Surf. Sci.* **277**, 337 (1992).
10. Maeland, A. J., Rittenhause, R., Lahar, W., and Romano, P. V., *Thin Solid Films* **21**, 67 (1974).
11. Mertens, F. P., *Surf. Sci.* **71**, 161 (1978).
12. Kaltchev, M. G., and Tysoe, W. T., *Surf. Sci.* **430**, 29 (1999).
13. Brenner, A., *J. Mol. Catal.* **5**, 157 (1979).
14. Davie, E., Whan, D. A., and Kemball, C., *J. Catal.* **24**, 272 (1972).
15. Smith, J., Howe, R. F., and Whan, D. A., *J. Catal.* **34**, 191 (1974).
16. Thomas, R., and Moulijn, J. A., *J. Mol. Catal.* **15**, 157 (1982).
17. Bartlett, B. F., Molero, H., and Tysoe, W. T., *J. Catal.* **167**, 470 (1997).
18. Olsthoom, A. A., and Moulijn, J. A., *J. Mol. Catal.* **8**, 147 (1980).
19. Brenner, A., and Burwell, R. L., Jr., *J. Am. Chem. Soc.* **97**, 2565 (1975).
20. Brenner, A., and Burwell, R. L., Jr., *J. Catal.* **52**, 353 (1978).
21. Howe, R. F., *Inorg. Chem.* **15**, 486 (1976).
22. Kazusaka, A., and Howe, R. F., *J. Mol. Catal.* **9**, 183 (1980).
23. Reddy, K. P., and Brown, T. L., *J. Am. Chem. Soc.* **117**, 2845 (1995).
24. Zecchina, A., Platero, E. E., and Areàn, C. O., *Inorg. Chem.* **27**, 102 (1988).
25. Gajda, G. J., and Weinberg, W. H., *J. Am. Chem. Soc.* **109**, 66 (1987).
26. Howe, R. F., and Leith, I. R., *J. Chem. Soc., Faraday Trans.* **169**, 1967 (1973).
27. Shirley, W. M., McGarvey, B. R., Maiti, B., Brenner, A., and Cichowlas, A., *J. Mol. Catal.* **29**, 259 (1985).
28. Wytenburg, W. J., and Lambert, R. M., *J. Vac. Sci. Technol. A* **10**, 3597 (1992).
29. Zaera, F., Kollin, E., and Gland, J. L., *Chem. Phys. Lett.* **121**, 415 (1985).
30. Kaltchev, M. G., Thompson, A., and Tysoe, W. T., *Surf. Sci.* **391**, 145 (1997).
31. Henrich, V. E., "The surface chemistry of metal oxides." Cambridge Univ. Press, Cambridge, 1994.
32. Kaltchev, M. G., and Tysoe, W. T., submitted for publication.
33. Mass Spectrometry Data Center, EPA MS number 156817, National Institute of Standards, Gaithersburg, MD, 2000.
34. Zecchina, A., Platero, E. E., and Areàn, C. O., *J. Catal.* **107**, 244 (1987).
35. Ballinger, T. H., and Yates, J. T., Jr., *Langmuir* **7**, 3041 (1991).
36. Braterman, P. S., "Metal Carbonyl Spectra," p. 180. Academic Press, New York, 1975.
37. Ang, H.-G., Chan, K.-S., Chuan, G.-K., Jaenicke, S., and Neu, S.-K., *J. Chem. Soc., Dalton Trans.* 3753 (1995).
38. Redhead, P. A., *Vacuum* **12**, 203 (1962).
39. Wagner, C. D., Riggs, W. M., Davis, L. E., Moulder, J. F., and Muilenberg, G. E., "Handbook of X-ray photoelectron spectroscopy." Perkin Elmer Corp., Eden Prairie, MN, 1979.
40. Quincy, R. B., Houalla, M., Proctor, A., and Hercules, D. M., *J. Phys. Chem.* **93**, 5882 (1989).
41. Quincy, R. B., Houalla, M., Proctor, A., and Hercules, D. M., *J. Phys. Chem.* **94**, 1520 (1990).
42. Yamada, M., Yasumarau, J., Houalla, M., and Hercules, D. M., *J. Phys. Chem.* **95**, 7037 (1991).
43. McGarvey, G. B., and Kasztelan, S., *J. Catal.* **148**, 149 (1994).
44. Hoffmann, F. M., Weisel, M. D., and Paul, J., *Surf. Sci.* **316**, 277 (1994).
45. Mascetti, J., and Tranquille, M., *J. Phys. Chem.* **92**, 2177 (1988).
46. Nakamoto, K., "Infrared and Raman spectra of inorganic and coordination compounds: Part B," 5th ed. Wiley, New York, 1997.
47. Fujita, J., Martelli, A. E., and Nakamoto, K., *J. Chem. Phys.* **36**, 339 (1962).
48. Ito, K., and Bernstein, H. J., *Can. J. Chem.* **34**, 170 (1956).
49. Kantschewa, M., Albano, G., Ertl, G., and Knözinger, H., *Appl. Catal.* **8**, 71 (1983).
50. Souter, P. F., and Andrews, L., *J. Am. Chem. Soc.* **119**, 7350 (1997).